A Forecast-Driven Stochastic Optimization Method for Proactive Activation of Manual Reserves

Julien Allard[1], Adriano Arrigo[1], Jérémie Bottieau[1], Gilles Bertrand[2], Zacharie De Grève[1] and François Vallée[1]
[1]Power Systems and Markets Research Group, University of Mons, Mons, Belgium
[2]Comission for the Regulation of Electricity and Gas, Brussels, Belgium

***Abstract*—Reducing operating balancing costs is paramount for an affordable transition towards renewable-dominated power systems. In European balancing markets, operating balancing costs are driven by the activation of automatic and manual frequency restoration reserves, respectively aFRR and mFRR. An inadequate combination of both products for resolving grid imbalances may result in economic inefficiencies where, e.g., saturated aFRR can lead to balancing price spikes. To avoid such situation, we propose a proactive activation policy of manual reserves, aiming at an optimal trade-off between aFRR and mFRR products via a stochastic optimization method. The tool is fed with 1-min time trajectories of system imbalances covering the next quarter hour. The one minute temporal granularity allows modeling the ramping phenomena of mFRR products, while keeping track of the faster activation of aFRR products. The proposed balancing energy activation methodology is tested on Belgian market data, which currently adopts a reactive balancing strategy. *Ex-post* comparisons of the proposed balancing strategy with a reactive one show that our methodology allows a decrease of the balancing activation costs. This is expected as early activation of mFRR, when appropriately provided, allows avoiding the activation of extremely high aFRR bids.**

***Index Terms*—Frequency restoration reserve, proactive activation, probabilistic forecasting, stochastic optimization.**

NOMENCLATURE

Sets and Indices

$s \in \mathcal{S}$	Set of system imbalance scenarios.
$t \in \mathcal{T}$	Set of time intervals.
$r \in \mathcal{R}_{a/m}^{U/D}$	Set of FRR bids (upward/downward).

Parameters

V_r	Volume of FRR bid [MW].
C_r	Price of FRR bid [€/MWh].
R_m	mFRR ramping rate [MW/min].
dt_a	aFRR control signal time step [h].
dt_m	mFRR control signal time step [h].
C_{ACE}	Cost associated to an area control error in the objective function [€/MWh].
π_s	Scenario probability.

Decision Variables

$a_{r,t,s}^{U/D}$	Activated aFRR volume [MW].
$m_{req,r}^{U/D}$	Activated mFRR volume [MW].
$m_{real,t}^{U/D}$	Real mFRR power supplied [MW].
$\Delta m_{t,+/-}^{U/D}$	mFRR power step [MW].
$ACE_{t,s}$	Area control error [MW].
$RS_{t+/-}^{U/D}$	Ramping start time interval (binary).
$z_{t,+/-}^{U/D}$	Ramping status (binary).

I. INTRODUCTION

Climate change concerns are driving European countries to significantly increase the penetration of renewable energy sources and thereby reduce greenhouse gas emissions [1]. The growing share of intermittent renewable sources along with the fast increase of the electricity demand due to the electrification of energy needs such as mobility and heating induce high levels of uncertainty. In this context, more flexibility sources are required by the system to dampen the potential consequences of uncertainty factors. Covering this need in a cost-optimal way is crucial if we wish not to dampen the efforts towards the actual transition of electricity systems.

In European balancing markets, frequency restoration reserves (FRR) are the principal mean for transmission system operators (traded through the PICASSO and MARI platforms) to restore the frequency [2]. Two types of FRR coexist, i.e., *i)* the automatic FRR (aFRR), which is continuously activated via controllers following a merit-order dispatch signal based on a real-time frequency error, and *ii)* the manual FRR (mFRR) characterized by a longer activation time (typically 12.5 minutes) and whose activation are subject to operator decisions[1].

Among the European transmission sytem operators (TSOs) there are several different policies for the activation of balancing energy [3]. Some countries, such as France, mainly rely on mFRR units with their large nuclear plants while others, such as Germany, activate aFRR units most of the time. Unfortunately, these policies might not be cost-efficient in all cases. In Belgium, for instance, expensive aFRR products may be activated while cheaper mFRR products remain available. Following a higher need for flexibility, the impact of cost-inefficient activation of aFRR and mFRR on society increases significantly, balancing costs being passed on the balancing responsible parties who themselves passed them on end-users. The activation of aFRR are automatic and based on control errors, widely accepted. Whereas, the activation of mFRR are

This work is financed through the ADABEL project.

[1]This work focus on the aFRR and mFRR considering the preliminary action of frequency containment reserve (FCR) in the balancing of the system.

more fuzzy, partly because the product is at the crossroad between reactive and proactive scheme.

Depending on the relative price differences between both products, a proactive activation of mFRR may result in potential cost savings for offsetting foreseen grid imbalances [4]. With respect to a reactive TSO's activation policy, the proactive activation of manual reserves necessitates to forecast the future needs in balancing services, and not only rely on the real-time control error signal [3].

In this line, this paper presents a stochastic model using probabilistic predictions of system imbalance for scheduling optimally early activation of mFRR minimising expected balancing costs. The proactive activation of manual reserves has already been addressed in the litterature. Particularly in [5], the authors propose a method to activate replacement reserves (RR) and manual reserves (mFRR) through sequentially cleared balancing markets based on a imbalance forecast. However, this paper does not quantify the potential savings for a TSO and it does not address the effects of forecast uncertainty on the benefits of the proposed method. In [6], regulation reserves (i.e., quick-start reserves, tertiary reserves - or mFRR, etc.) are optimally scheduled through a multi-objective optimisation problem with a cost function aiming at maintaining the power balance at a minimal cost. They perform the optimisation on a rolling horizon with a deterministic system imbalance scenario. Although they observed balancing costs savings, they highlight the impact of the prediction error on the amount of activated aFRR which can be a more dynamic but expensive product in some countries. Reference [7] significantly improves the aforementioned works as it proposed a stochastic optimisation problem to schedule aFRR and mFRR products in a cost optimal way taking into account forecast errors, but the use case definition miss the potential savings behind the proactive activation of mFRR as the bid prices are set lower for mFRR products than aFRR ones.

The methods for the activation of FRR reserves, proposed in the aforementioned works, either include the system imbalance forecast or a stochastic formulation of the optimisation problem but never both at once. In this paper, we go beyond by proposing a full probabilistic prediction - scenario-based decision chain to address the problem of proactive activation of mFRR reserves and validating this results with real data to quantify the benefits of the method. The main contributions of this paper are the following:

- we derive a tool that generates a probabilistic forecast of the future system imbalance over one quarter of an hour,
- we formulate the proactive activation of mFRR products through a stochastic optimization methodology.

We perform a cost-benefit analysis, based on real Belgian data, and investigate the dependence of the attainable cost reduction on the accuracy of the system imbalance forecast.

The remainder of the paper is organized as follows. Section 2 compares the current activation policy of FRRs products in Belgium to a simple version of the methodology proposed in Section 3. This particular section describes the prediction tool and the formulation of the stochastic optimization problem. Section 4 presents the main results in terms of economic and balancing performances. Conclusions are drawn in the final section.

II. Activation of aFRR and mFRR: Current Belgian Regulatory Framework

In this section, we introduce the current practice for the activation of FRRs in Belgium, and put it into perspective with a naïve alternative approach (inspired by our proposed methodology in Section III) highlighting the benefits of making the trade-off between aFRR and mFRR bids for the activation of FRR.

These two types of FRR diverge in terms of time response and activation procedure as aFRR is continuously activated via controllers based on a real-time frequency error, and mFRR is manually activated by the operator with a longer activation time (typically 12.5 minutes). In Belgium FRR products are activated based on the following methodology. After the imbalance netting process (IGCC), the activation of aFRR is based on a merit order mechanism constituted of the aFRR energy bids for the concerned quarter of an hour. The decision is taken every 4 seconds by the aFFR controller that also calculates the control targets, i.e. volumes requested per energy bid. The mFRR activation decision is taken based on the system imbalance of the 10 previous minutes (minimum) and the level of activated aFRR. The goal of manual reserves is to avoid out-of-range area control error and to alleviate the automatic ones. The activated mFRR energy bids are also activated according to a merit order mechanism that additionally considers technical properties of the bids. The requested mFRR volume holds for the entire quarter of an hour.

A similar simplified activation policy is used as benchmark for the evaluation of the proposed approach. This policy, called *Actual Policy* in Fig.1 and in the remaining of the paper, implies that the system imbalance is firstly covered by aFRR based on the merit order principle and that mFRR solely compensates residual imbalance when the automatic reserves do not compensate it all.

Nowadays, this practice for activating FRRs resources may not be the most cost-efficient. Indeed, aFRR bid prices tend to increase fostered by their priority activation. Despite their high prices, aFRR volumes are activated while cheaper mFRR volumes could be activated instead. For instance, over the year 2022, during each quarter of an hour, 900 MW of mFRR bids had a cheaper activation price than 60 MW of aFRR bids on average in Belgium. In this framework, putting in perspective aFRR and mFRR bids to decide the balancing actions could reduce the balancing activation costs. Such potential cost savings can be observed from the balancing bids submitted in 2022. Assuming perfect information on the future system imbalance (SI), Fig.1 shows that identifying the best interplay between mFRR and aFRR products (similar dynamic considered for the sake of simplicity) achieves a 35% decrease

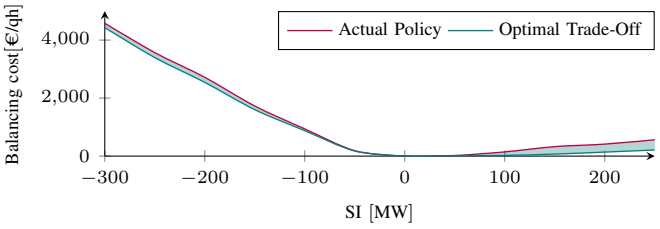

Fig. 1. Average balancing costs per quarter-hour over the year 2022

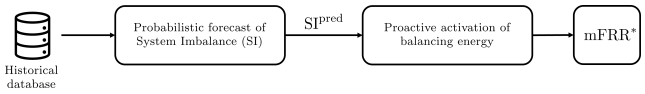

Fig. 2. Flowchart of the forecast-driven proactive activation tool of mFRR balancing services.

in terms of balancing cost compared to the simplified actual policy.

Those preliminary results, even though they carry a key message, are upper cost savings limits. aFRR and mFRR products do not have the same dynamic behaviour, aFRR products being able to respond much faster as described previously. However, with a proactive activation of mFRR volumes TSOs could anticipate their ramping period and optimize the balancing action. Hence, the remaining of this work propose a stochastic *Proactive Policy* for the activation of mFRR reserves.

III. Forecast-Driven Proactive Activation Tool

The overall methodology for activating proactively volumes of mFRR reserves under uncertainty is layout in Fig. 2. This methodology is divided into two blocks, i.e., one about the generation of 1-min time trajectories of system imbalances[2], and the other one about the actual proactive provision of mFRR balancing energy. Accordingly, section III-A details the first block of the overall methodology, while section III-B details the proactive balancing cost minimization problem faced by the TSO.

A. Prediction of 1-min time trajectories of System Imbalance

The approach for generating 1-min time trajectories of system imbalances is composed of two steps, one producing scenarios of 15-min averaged system imbalances, and a second step for deriving 1-min time trajectories of system imbalance for each drawn scenarios. System imbalance prediction is known to be a hard task already for 15-min average values, and this difficulty gets worse when inferring its intra quarter hour dynamic behavior. Hence, predicting directly 1-min time trajectories of system imbalances might be a too noisy process to infer, and we thus prefer here decomposing the prediction task into two steps. Fig. 3 exemplifies this two-step approach, where three 15-min system imbalance scenarios are randomly

[2]Note that, in our case, we retrieve the imbalance netting contribution of neighboring countries from the system imbalance.

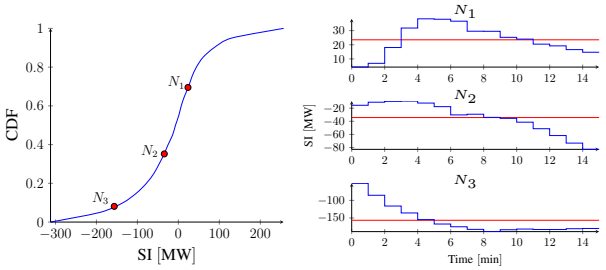

Fig. 3. Prediction example of three 1-min time trajectories of System Imbalance. On the right-hand side figures, the red lines represent the 15-min system imbalance scenarios and the blue lines represent the 1-min nearest neighbour trajectories.

picked from a forecasted cumulative distribution function (f-CDF) (shown on the left-hand-side of Fig. 3). Each scenario is then mapped with a 1-min time trajectories via a nearest neighbor method (as observed in the right-hand-side of Fig. 3).

The forecasted CDF is obtained using a spline cubic interpolation between predicted quantiles. The quantile forecasts are outputted by an advanced neural architecture based on the Transformer architecture which is trained offline [8], [9], [10]. This deep learning model emerge as one of the best approaches for forecasting real-time market variables, as exemplified by [8] and [11]. More particularly, a set of quantile prediction (ranging from the 1-percentile to the 99-percentile in steps of 5) are generated at the beginning of each quarter hour in a rolling window approach. The inputs are time series observed on previous quarter hours, and future information available over the next quarter hour. More specifically, times series observed consist of previously measurements of, e.g., system imbalance, activated balancing services, or the netted physical exchanges of Belgium with neighbouring countries over a look-ahead horizon, while future information primarily concerns calendar information, the schedules of power units, and forecasted wind and photovoltaics powers over the next quarter hour.

After a uniform random sampling of N_S scenarios from the f-CDF (being thus of equal probability π_s), each 15-min scenario of system imbalance is mapped with a 1-min time trajectory of system imbalance. This mapping is performed via the nearest neighbor approach. Practically, the nearest neighbor approach ranks all 1-min time trajectories of system imbalance contained in a historical database based on the similarity of their average value w.r.t. the 15-min scenario, and directly forwards the closest one.

B. Proactive Activation of mFRR

The generated scenarios are used by the stochastic optimisation model to compute the optimal volume of mFRR that should proactively be activated to minimise the balancing activation costs and the area control error. The problem models the operational behaviour of the aFRR and mFRR products in the balancing process. The full formulation of the problem is presented in the following.

1) Objective Function: Finally the objective is to minimise the area control error and balance the system at minimum costs.

$$Costs_s = \sum_r (C^U_{mFRR,r} m^U_{req,r} + C^D_{mFRR,r} m^D_{req,r}) dt_m + \sum_r \sum_t (C^U_{aFRR,r} a^U_{r,t,s} + C^D_{aFRR,r} a^D_{r,t,s}) dt_a \quad (1)$$

The FRR products are activated according to the prices of aFRR, $C^{U/D}_{aFRR,r}$, and mFRR, $C^{U/D}_{mFRR,r}$, bids submitted on the balancing market via market order mechanism. The balancing services providers are remunerated on a pay-as-bid principle considering the requested volume of aFRR and mFRR. Consequently, (1) defines the balancing costs structure.

The resulting scenario-based proactive activation of mFRR problem writes as[3]

$$\min_{\Omega} \sum_s \pi_s (C_{ACE} \sum_t (|ACE_{t,s}| dt_a) + Costs_s) \quad (2)$$

s.t. aFRR Constraints (1) - (2)
mFRR Constraints (3)- (18)
Balancing Constraint (19)
Costs Constraint (20)

with $\Omega = \{a^{U/D}_{r,t,s}, m^{U/D}_{req,r}, m^{U/D}_{real,t}, \Delta m^{U/D}_{t,+/-}, ACE_{t,s}, RS^{D/U}_{t,+/-}, z^{U/D}_{t,+/-}\}$ the set of decision variables. In (2), C_{ACE} represents the cost associated with an area control error. It is set slightly higher than the most expensive FRR bid such that every bid could be activated, considering the balancing task more crucial than economical savings. The absolute value in (2) is linearized by decomposing the area control error into its positive and negative component $ACE_{t,s} = ACE^+_{t,s} - ACE^-_{t,s}$ and reformulating the absolute value, $|ACE_{t,s}| = ACE^+_{t,s} + ACE^-_{t,s}$. Big-M constraints are used to ensure that the two components are mutually exclusive as for linearizing the bilinear terms in (5) and (21) [12]. This problem can therefore be formulated as a mixed-integer linear program (MILP) problem that can be solved efficiently using off-the-shelve solver (Gurobi) which implements the branch-and-bound algorithm.

2) Balancing constraint: The aFRR and mFRR reserves are activated in order to compensate the system imbalance of the system and consequently, restore the frequency.

$$ACE_{t,s} = SI_{t,s} + \sum_{r \in \mathcal{R}^U_a} a^U_{r,t,s} - \sum_{r \in \mathcal{R}^D_a} a^D_{r,t,s} + m^U_{real,t} - m^D_{real,t} \quad \forall t \in \mathcal{T}, \forall s \in \mathcal{S} \quad (3)$$

The remaining imbalance or area control error (ACE) is the sum of the system imbalance and the net regulation volume, i.e. net aFRR and mFRR volumes activated. (3) is defined for all N_S sampled system imbalance profiles during the quarter hour of interest, qh. However, for the previous quarter, $qh-1$, a single scenario that is the median of the CDF generated at the beginning of this particular quarter (i.e., 15 minutes before the quarter qh) is considered.

[3]Note that the data used in the numerical study of Section IV is anonymized and it is therefore not possible to consider network constraints which may impact the activation decisions to avoid congestion.

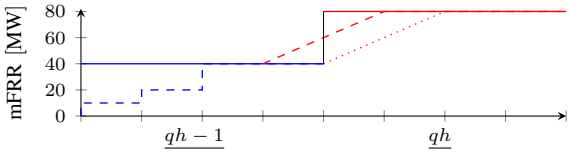

t	-3	-2	-1	0	1	2	3	4
RS^A	0	0	0	1	0	-	-	-
z^A	-	-	-	1	1	0	0	0
RS^B	0	0	0	0	1	-	-	-
z^B	-	-	-	1	1	1	0	0

Fig. 4. Example of mFRR units ramping variables states with T = 4. Plain line are for requested mFRR volumes and dashed/dotted lines are the real supplied power curve (blue = $qh-1$ and red = qh).

3) Manual Frequency Restoration Reserves: In this model, two mFRR signals are distinguished: the requested mFRR volumes, $m^{U/D}_{req,r}$, and the mFRR power really delivered to the system, $m^{U/D}_{real,r}$. Indeed, if each requested volume holds for 15 minutes, dt_m, mFRR products have a slower reaction time and are subject to ramping constraints.

$$0 \leq m^{U/D}_{req,r} \leq V^{U/D}_{mFRR,r} \quad \forall r \in \mathcal{R}^{U/D}_m \quad (4)$$

$$m^U_{req,r} m^D_{req,r} = 0 \quad \forall r \in \mathcal{R}^{U/D}_m \quad (5)$$

The mFRR requested volumes, similarly to aFRR ones, are positive and limited by the submitted bids volumes, $V^{U/D}_{mFRR,r}$, in (4) and upward and downward reserves can not be activated during the same quarter of an hour thanks to (5).

The real power delivered by the mFRR reserves, $m^{U/D}_{real,r}$, follows the request but transitions between two requested levels are constrained by a fixed ramping rate, R_m, in both directions. In the proposed proactive policy, mFRR units can start ramping during the previous period, $qh-1$, as shown in Fig.4. The real power delivered during this quarter hour, i.e., the total mFRR power is considered as all units have a common ramping rate, is defined over two quarters: the quarter of an hour for which the optimal mFRR set point is computed, qh and the previous quarter during which the ramping might start, $qh-1$.

$$\sum_{t=1}^{T+1} RS^{D/U}_{t,+} + RS^{D/U}_{t,-} = 1 \quad \forall t \in \mathcal{T} \quad (6)$$

$$\sum_{t=1}^{T+1} RS^{D}_{t,+} + RS^{U}_{t,+} = 1 \quad \forall t \in \mathcal{T} \quad (7)$$

$$\sum_{t=1}^{T+1} RS^{D}_{t,-} + RS^{U}_{t,-} = 1 \quad \forall t \in \mathcal{T} \quad (8)$$

$$RS^{D/U}_{t,+/-} \in \{0,1\} \quad \forall t \in \mathcal{T} \quad (9)$$

Equation (9) introduces binary variables, $RS^{D/U}_{t,+}$, that take a value of 1 when the mFRR units start ramping. Equation

(6) ensures that neither upward nor downward reserves receive ramping start signals in both directions during the same quarter hour. Equations (7)-(8) also constraint upward and downward products to not ramp in the same direction.

$$\Delta m^{U/D}_{t,+/-} = R_m \sum_{\tau=1}^{t+T} RS^{D/U}_{\tau,+/-} \quad \forall t = -T+1:0 \tag{10}$$

$$m^{U/D}_{real,-T+1} = m^{U/D}_{prev,1} + \Delta m^{U/D}_{-T+1,+} - \Delta m^{U/D}_{-T+1,-} \tag{11}$$

$$\begin{aligned} m^{U/D}_{real,t} = m^{U/D}_{real,t-1} + m^{U/D}_{prev,t} - m^{U/D}_{prev,t-1} \\ + \Delta m^{U/D}_{t,+} - \Delta m^{U/D}_{t,-} \quad \forall t = -T+2:0 \end{aligned} \tag{12}$$

If mFRR units start ramping during the previous period, (10) fixes the power variation, $\Delta m^{U/D}_{t,+/-}$, to R_m. This variation comes on top of the already activated volumes that follow the control signal sent 15 minutes earlier. The real power delivered during the previous quarter of an hour is modified as expressed in (11)-(12), where $m^{U/D}_{prev,t}$ is the power that was expected to be delivered during the previous quarter, $qh-1$, when computing the requested mFRR volume during this particular quarter.

$$\Delta m^{U/D}_{t,+/-} \geq z^{U/D}_{t+1,+/-} R_m \quad \forall t = 1:T \tag{13}$$

$$\Delta m^{U/D}_{t,+/-} \leq z^{U/D}_{t,+/-} R_m \quad \forall t = 1:T \tag{14}$$

$$z^{U/D}_{t+1,+/-} \leq z^{U/D}_{t,+/-} \quad \forall t = 1:T \tag{15}$$

$$z^{U/D}_{0,+/-} = \sum_{t=1}^{T+1} RS^{D/U}_{t,+/-} \tag{16}$$

$$m^{U/D}_{real,t} = m^{U/D}_{real,t-1} + \Delta m^{U/D}_{t,+} - \Delta m^{U/D}_{t,-} \quad \forall t = 1:T \tag{17}$$

$$z^{U/D}_{t,+/-} \in \{0,1\} \quad \forall t = 0:T \tag{18}$$

During the quarter of interest, qh, the ramping may continue until the requested level is reached. (18) introduces other binary variables defined during the concerned quarter of an hour, qh, that represents the ramping rate status of upward and downward reserves. (13)-(16) ensure that as long as the power varies the ramping rate stays constant. The power really supplied by mFRR units evolves as expressed in (17).

$$\sum_{t=1-T}^{T} \Delta m^{U/D}_{t,+/-} = \sum_{r \in \mathcal{R}^{U/D}_m} mFRR^{U/D}_{req,r} - mFRR^{U/D}_{req,prev} \tag{19}$$

The transition between the total previously requested mFRR volume, $mFRR^{U/D}_{req,prev}$, and the total requested mFRR volume, $mFRR^{U/D}_{req,r}$, must be finished before the end of the concerned period. That is to say that the total mFRR power variation over the two quarters, $qh-1$ and qh, must be equal to the difference between the requested mFRR volume of those two quarters as written in (19).

4) Automatic Frequency Restoration Reserves: The aFRR products are modelled with a 1 minute resolution, dt_a. Although both reserves are subject to ramping time limit, only mFRR ramping constraints are modelled throughout this paper given the faster reaction of aFRR controller.

$$0 \leq a^{U/D}_{r,t,s} \leq V^{U/D}_{aFRR,r} \quad \forall r \in \mathcal{R}^{U/D}_a, \forall t \in \mathcal{T}, \forall s \in \mathcal{S} \tag{20}$$

$$a^{U}_{r,t,s} a^{D}_{r,t,s} = 0 \quad \forall r \in \mathcal{R}^{U/D}_a, \forall t \in \mathcal{T}, \forall s \in \mathcal{S} \tag{21}$$

The amount of activated aFRR, $a^{U/D}_{r,t,s}$, is positive and limited by the available volumes submitted to the TSO, $V^{U/D}_{aFRR,r}$, in (20). Simultaneous activation of upward and downward products, which might occur when some bid prices are negative (i.e., potential revenues generated by playing in both directions), via (21).

IV. Numerical Simulations

Three balancing energy activation strategies are tested and compared: (1) a reactive balancing energy policy, i.e., mFRR are actived only in case of saturation of aFRR, (2) an optimal FRR products trade-off (showcased in section II), and (3) our proposed forecast-driven proactive activation policy. The decision to activate mFRR is made at the beginning of the quarter hour for the approaches (1) and (2), while this decision is performed 15 min before for the approach (3). Regarding the forecasts of system imbalance, (1) and (2) employs a deterministic approach, where the 1-min trajectory is obtained using the median of the predicted CDF, while (3) considers a set of 1-min trajectories derived by sampling the predicted CDF.

Those three strategies are implemented on a Belgian case study and compared over each quarter hour of one year. Notably, data are collected from the Belgian's TSO (Elia) website [13]. For the prediction of the 1-min time trajectories of system imbalance, the data covering the period 2016-2021 is exploited as training and validation sets for the deep learning model and as historical database for the nearest neighbor approach. The year 2022 is used as a test set. aFRR and mFRR bids, volumes and prices, are also gathered via the Elia website. In practice, the ramping rate has a lower bound requiring that the bid volume is fully activated in 15 minutes. However, in the proposed formulation of the problem bids might be discriminated based on their ramping rate limit as the area control error has the biggest weight in the objective function. Bids with faster ramping performances could be activated by the decision tool even with higher prices while the method aims at selecting the bids according to the prices. Therefore, the ramping rate is fixed, for upward and downward reserves and in both directions, to 250 MW per 15 minutes, corresponding to the 0.95 quantile of the activated mFRR volumes without ramping constraints.

The comparison is performed by applying *ex-post* the optimal activated mFRR volumes to the true system imbalance realisation, i.e. determine the optimal activation of aFRR volumes considering the real imbalance while keeping the value for the mFRR products requested by the prediction-decision chain. The balancing energy activation strategies are compared in terms of activation costs, balancing volumes and

TABLE I
EXAMPLE: BALANCING STRATEGIES RESULTS FOR THE TWO PERIODS

Activation Strategy	FRR Costs [€/MWh]	|ACE| [MW]
Actual Policy	97.9/110.2	115/110
Optimal Trade-Off	110.6/116.1	75.5/76
Proactive Policy	99.4/126.6	0.6/0

area control error, i.e., the remaining system imbalance error after TSO balancing actions.

A. Discussion on the results of the three strategies

First, the principle of the different balancing energy activation strategies is illustrated on two periods in Fig. 6 and the associated results are presented in Table I. We can see that the strategy (1) (top graph) mainly activates aFRR units, but as the aFRR volumes limits are reached some mFRR volumes are also requested. However, even if the average costs of the activated units may be lower than for the two other strategies for the firs period, the average area control error are significantly higher during the two periods if activated reserves are selected sequentially. Indeed, strategy (2) improves the previous one by activating a bit more mFRR reserves considering the bid prices of both aFRR and mFRR products. Finally, the proposed forecast-driven proactive strategy (3), further improves the balancing action by allowing to ramp during the previous period. For the two periods, the strategy (3) has the best objective function value.

Statistical information on the performances of the three balancing energy activation strategies are presented in Fig. 5. This figure shows the positive effects of considering both aFRR and mFRR bids a quarter ahead (3) compared to a reactive balancing policy (1). It avoids high FRR activation costs when the system imbalance is high and the last aFRR bids are expensive. It furthermore reduces the area control error most of the time. This is also the case for the optimal trade-off strategy (2). An optimal interplay between aFRR and mFRR products already improves in many aspects the actual policy benchmark (1) in terms of FRR costs and area control error. Nevertheless, Fig. 5 allows assessing the impact of forecast errors on the performances of the proposed activation policy of FRR. Indeed, forecast made at the beginning of the quarter of an hour are used in strategy (1) and (2), while forecast made one quarter hour ahead feeds the strategy (3). Interestingly, a proactive activation of mFRR reserves further reduces the FRR activation costs while increasing the amount of activated reserves. This may be due to the fact that ramping trajectories of mFRR are not remunerated. As the system imbalance may exhibits a significant auto-correlation, ramping mFRR may also help the system for those quarter hours. However, the additional FRR volumes activated seem to be more consequent than the reduction of the area control error. Indeed, forecast errors may have a negative impact on the proactive activation of the reserves as the ramping decisions also affect the real activated volumes of the previous quarter of an hour. This may lead to the activation of more aFRR to compensate a non-optimal activation of mFRR reserves. The impacts of forecast errors are discussed in the following section.

B. Forecast performances and its impacts on the activation of mFRR

First, we evaluate the performance of the predicted imbalance trajectories (used in strategy (3)) by using the Continuous Ranked Probability Score (CRPS) [14]. Fig. 7(a) presents the CRPS values in blue at both 15-minute (dashed line) and 1-minute (solid line) time resolution. These results are compared with a naive forecasting approach (showed in black in Fig. 7(a)), which randomly selects system imbalance values based on the historical system imbalance CDF. As illustrated in Fig. 7(a), the proposed forecasting tool outperforms the naive method in both time resolution. More particularly, regarding the 15-minute resolution forecasts, the transition observed in the dashed blue line across the two quarter-hour intervals highlights the challenge in being accurate for system imbalance prediction as the prediction horizon extends. This is illustrated by the performance gap between the proposed forecasting tool and the naive approach shifting from 13% to 5% across both quarter hours. In the context of 1-minute resolution forecasts, we can observe that, for both predicted quarter hours, there is an increase in uncertainty during the initial minutes compared to the latter ones. This observed behavior might be due to the imbalance settlement period's design, which operates on a 15-minute time resolution. The transition between imbalance settlement periods can trigger significant ramps in both power supply and demand, which render the dynamics of the early minutes of each quarter hour especially unpredictable. Additionally, we compare the performance of the forecasting approaches used in strategies (2) and (3). Given that strategy (2) uses a deterministic forecast, we calculate the absolute errors (AE) over the year 2022, as it is the equivalent of CRPS for deterministic forecasts [14]. Fig. 7(b) showcases the distributions of CRPS and AE throughout the year 2022. On average, the CRPS score for strategy (3) is at 84 MW, while the MAE for strategy (2) is at 100 MW. Although the forecasts for strategy (3) are produced 15 minutes ahead of time compared to those for strategy (2), the probabilistic approach helps to mitigate the potential disadvantages of an extended forecasting horizon. Going a step further into strategy (3), Fig. 7(c) shows the impact of forecasting errors on the activation of mFRR. Overall, the global trend is reasonable, showing that mFRR tend to be activated in opposition with the observed system imbalance (which are represented by points falling into the upper left and lower right quadrants). However, the presence of points in the upper right and lower left quadrants indicates that mFRR have been inappropriately activated, aggravating rather than correcting the system imbalance. Such forecast errors, highlighted by high CRPS values, suggest potential benefits for exploring risk-aware approaches in the activation of mFRR.

In the same context, Fig. 7(d) and Fig. 7(e) shows impact of suboptimal mFRR activation on the two aspects of the objective function: the Area Control Error (ACE) and the

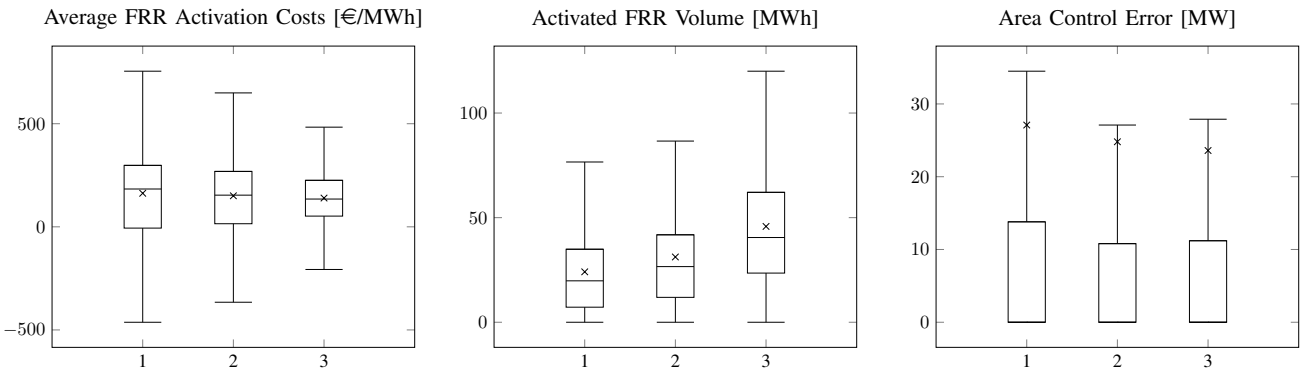

Fig. 5. Results comparison: (1) Actual Policy - (2) Optimal FRR Trade-Off - (3) Proactive Policy

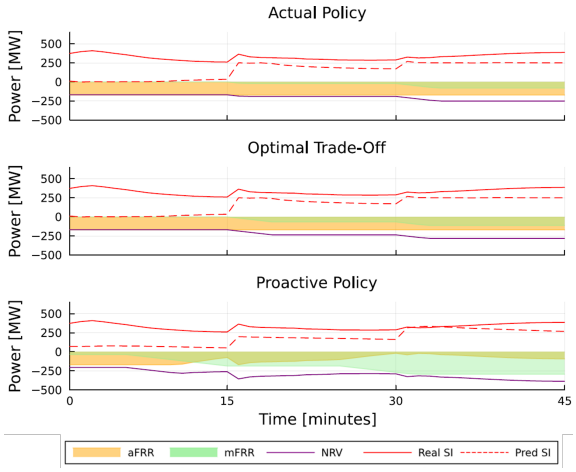

Fig. 6. Balancing energy activation results for the three different strategies on two periods.

total balancing costs. In Fig. 7(d), the upper right and lower left display particularly high ACE values. This occurs when aFRR are insufficient to counteract the badly activated mFRR driven by inaccurate SI predictions. Fig. 7(f) accentuates this observation with a heatmap that tracks the activation of aFRR, which shows an increased use of aFRR in both quadrants. Additionally, this figure indicates that when the observed system imbalance is around zero, aFRR products are typically the most cost-effective and, thus, the preferred choice for activation. Interestingly, Fig. 7(e) reveals that substantial activations of mFRR (extreme values in upper left and lower right) can result in reasonable balancing costs (as indicated by the shift towards white on the heatmap). These extreme points illustrate the potential cost-effectiveness of preemptively activating mFRR for balancing the system. Of course, the cost disparity observed between negative and positive system imbalance stems primarily from the bid structure of the balancing offers, rather than from forecasting errors, upward reserves being typically priced higher than downward reserves.

C. Sensitivity Analysis

For each quarter of an hour, several system imbalance scenarios are sampled to represent the future system imbalance.

TABLE II
OPTIMAL TRADE-OFF SCENARIO-BASED METHOD ON THE FIRST DAY OF 2022

	$N_S = 10$	$N_S = 20$	$N_S = 50$	$N_S = 100$
Time [s/qh]	0.288	0.575	1.313	4.35
Objective [€]	8790	5569	5223	4583

The number of scenarios must be chosen carefully to unlock the full potential of the method. In this work, we decided to take 20 scenarios for each quarter of an hour by making a trade-off between the best objective value and the computation time (i.e., a full year being simulated at once). However, a sensitivity analysis on the number of scenarios (N_S) has been carried out on the first day of the year 2022. The 96 quarter-hours of the day has been simulated for 10, 20, 50 and 100 system imbalance scenarios and to mitigate bias in the results, for each case and each quarter-hour, several scenarios samplings have been done until convergence of the average objective value. Obtained results can be seen in Tab. II. We can observe that, for operational use, increasing the number of scenarios may have a significant impact on the objective within an acceptable timeframe.

V. CONCLUSION

This paper develops a full probabilistic prediction - scenario-based decision chain to address the proactive activation of mFRR reserves in a cost-efficient balancing strategy. The chain includes a tool that generates a probabilistic forecast of the future system imbalance and a stochastic optimization formulation of proactive activation of mFRR.

Using this model we show that an appropriate trade-off between aFRR and mFRR products avoid the activation of high prices aFRR bids when cheapest mFRR units are available in case of extreme system imbalance. This helps to reduce the average balancing activation costs which is of major importance in the current situation where the predictability of generation and consumption becomes harder and that more balancing actions are requested. Results also shows the improved benefits through the proactive activation of mFRR, anticipating the ramping period and by doing so, further reducing the activation

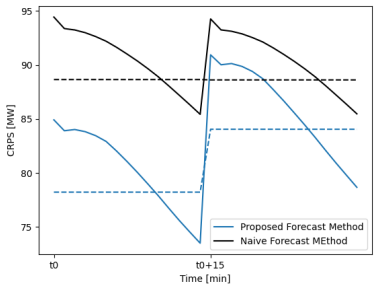

(a) Average CRPS results over the year 2022 for both the proposed (blue) and naive (black) forecasting approaches. Dashed lines represent the 15-minute resolution, while solid linex represent the 1-minute resolution.

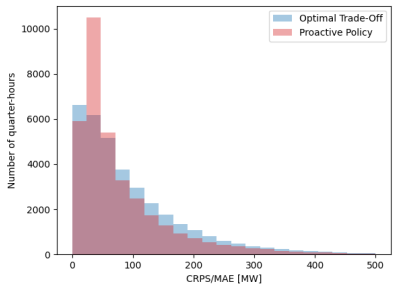

(b) Distributions of i) the CRPS of probabilistic forecasts used in the stochastic proactive policy (in red) and ii) the AE of deterministic forecasts used in the deterministic optimal trade-off (in blue) over the year 2022.

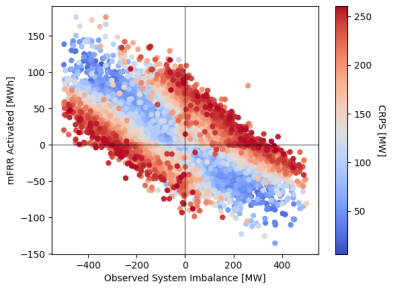

(c) CRPS with respect to the proactive strategy's mFRR activations and observed system imbalance scenarios for 2022.

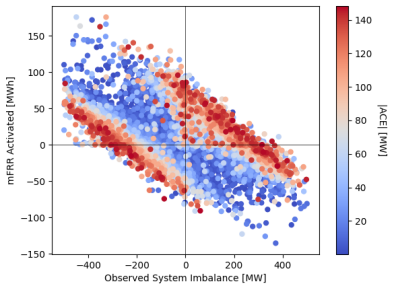

(d) Absolute average area control error with respect to the proactive strategy's mFRR activations and observed system imbalance scenarios for 2022.

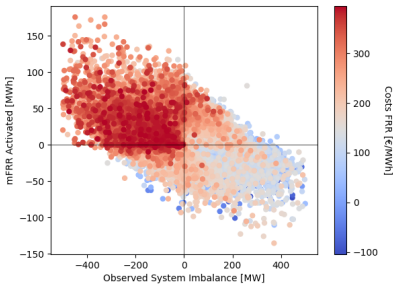

(e) Average FRR (aFRR and mFRR) cost with respect to the proactive strategy's mFRR activations and observed system imbalance scenarios for 2022.

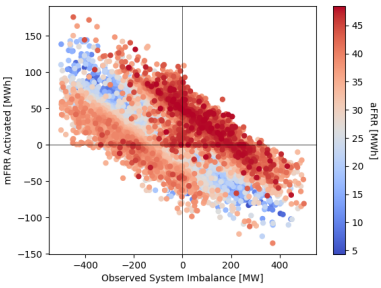

(f) Activated aFRR volume in real-time with respect to the proactive strategy's mFRR activations and observed system imbalance scenarios for 2022.

Fig. 7. Forecast performances and prediction error impact on the results.

costs while confining the area control error level. However, the proposed methodology is sensitive to prediction errors and might therefore request the activation of more FRR volumes, additional aFRR volumes being used to compensate inefficient mFRR activation.

Therefore, this work may be improved by using the probabilistic prediction - scenario-based decision chain on a rolling horizon, updating the decision to start ramping and the requested mFRR volumes over time. We might also be interested to improve the forecasting tool by taking the k-closest neighbours to define the 1 minute time step system imbalance trajectories.

References

[1] European Court of Auditors, "EU climate and energy targets," Tech. Rep., 2023.

[2] R. Mieth, Y. Dvorkin, and M. A. Ortega-Vazquez, "Risk-aware dimensioning and procurement of contingency reserve," *IEEE Transactions on Power Systems*, vol. 38, no. 2, pp. 1081–1093, 2023.

[3] M. Håberg and G. Doorman, "Classification of balancing markets based on different activation philosophies: Proactive and reactive designs," in *International Conference on the European Energy Market, EEM*, vol. 2016-July. IEEE Computer Society, 7 2016.

[4] P. Shinde, M. R. Hesamzadeh, P. Date, and D. W. Bunn, "Optimal dispatch in a balancing market with intermittent renewable generation," *IEEE Transactions on Power Systems*, vol. 36, no. 2, pp. 865–878, 2021.

[5] M. Håberg and G. Doorman, "Proactive planning and activation of manual reserves in sequentially cleared balancing markets," in *Proceedings of IEEE EPEC 2017*, 2017, pp. 1–6.

[6] H. Petr and M. Ondrej, "Optimal dispatch of regulation reserves for power balance control in transmission system," in *IEEE International Conference on Control and Automation*. IEEE, 2009, pp. 807–812.

[7] M. Håberg and G. Doorman, "A stochastic mixed integer linear programming formulation for the balancing energy activation problem under uncertainty," in *2017 IEEE Manchester PowerTech*, 2017, pp. 1–6.

[8] J. Bottieau, Y. Wang, Z. De Grève, F. Vallée, and J.-F. Toubeau, "Interpretable transformer model for capturing regime switching effects of real-time electricity prices," *IEEE Transactions on Power Systems*, vol. 38, no. 3, pp. 2162–2176, 2023.

[9] J.-F. Toubeau, J. Bottieau, Y. Wang, and F. Vallée, "Interpretable probabilistic forecasting of imbalances in renewable-dominated electricity systems," *IEEE Transactions on Sustainable Energy*, vol. 13, no. 2, pp. 1267–1277, 2022.

[10] J. Bottieau, L. Hubert, Z. De Grève, F. Vallée, and J.-F. Toubeau, "Very-short-term probabilistic forecasting for a risk-aware participation in the single price imbalance settlement," *IEEE Transactions on Power Systems*, vol. 35, no. 2, pp. 1218–1230, 2020.

[11] V. N. Ganesh and D. Bunn, "Forecasting imbalance price densities with statistical methods and neural networks," *IEEE Trans. Energy Markets, Policy and Regulation*, pp. 1–10, 2023.

[12] J. Fortuny-Amat and B. McCarl, "A Representation and Economic Interpretation of a Two-Level Programming Problem," *Journal of the Operational Research Society*, vol. 32, no. 9, pp. 783–792, 1981.

[13] OpenDataElia, "Open data," https://opendata.elia.be/pages/home/, Accessed on 2023-09-20.

[14] T. Gneiting and A. E. Raftery, "Strictly proper scoring rules, prediction, and estimation," *Journal of the American Statistical Association*, vol. 102, no. 477, pp. 359–378, 2007.